Available online at www.sciencedirect.com

ScienceDirect

Energy Procedia 158 (2019) 4870–4881

Energy Procedia

www.elsevier.com/locate/procedia

10th International Conference on Applied Energy (ICAE2018), 22-25 August 2018, Hong Kong, China

Low-temperature carbonatization of metal oxides

Danny Müller[a,*], Christian Knoll[a,b], Georg Gravogl,[a,c] Werner Artner[d], Andreas Werner[e], Jan M. Welch,[f] Michael Harasek[b], Ronald Miletich,[c] Peter Weinberger[a]

[a] *Institute of Applied Synthetic Chemistry, TU Wien, Getreidemarkt 9, 1060 Vienna, Austria.*
[b] *Institute of Chemical, Environmental & Biological Engineering, TU Wien, Getreidemarkt 9, 1060 Vienna, Austria.*
[c] *Institut für Mineralogie und Kristallographie, University of Vienna, Althanstraße 14, 1090 Vienna, Austria*
[d] *X-Ray Center, TU Wien, Getreidemarkt 9, 1060 Vienna, Austria.*
[e] *Institute for Energy Systems and Thermodynamics, TU Wien, Getreidemarkt 9, 1060 Vienna, Austria.*
[f] *Atominstitut, TU Wien, Stadionallee 2, 1020 Vienna, Austria.*

Abstract

In the present work carbonatization of selected metal oxides was investigated at temperatures below 100 °C and CO_2 pressures of 1-55 bar (25 °C) and 110 bar (60 °C) by *in-situ* powder diffraction, as well as experiments in a pressure reactor. Moisture was confirmed to be a crucial requirement for any successful carbonatization, as under dry conditions always the initial metal oxide was recovered. Under the applied conditions a successful carbonatization of CaO, MnO, ZnO, CoO and PbO was achieved, highlighting, that although commonly studied at high temperatures, carbonatization of metal oxides can also be successfully operated in the presence of moisture with an elevated CO_2 pressure as driving force.

Keywords: metal oxides; low-temperature carbonatization; non-ambient conditions; *in-situ* P-XRD; thermochemical energy storage

1. Introduction

In the recent past, the excessive use of fossil fuels to satisfy global energy demands has resulted in increased awareness, not only of their limited availability but also the associated increase in anthropogenic atmospheric CO_2. Whereas the limited availability stimulated the research on alternative energy sources and energy efficiency [1], the increased CO_2 release gave rise to political measures restricting CO_2 emissions [2, 3], as well as to ambitious research programs on CO_2 fixation. [4]

One major issue is that power plants continue to be operated with fossil fuels. Measures dealing with this topic target avoidance of CO_2 release, its separation from flue gas or other gases and subsequent storage as form of

10.1016/j.egypro.2019.01.706

deposition. The avoidance of CO_2 release is hampered by the economic attractiveness of fossil fuel power plants. Therefore, as compromise research on an effective separation and subsequent storage or conversion of CO_2 from flue gas has intensified. In this context, separation of CO_2 incurs notable financial penalties for power plant and a concomitant reduction of energy output. [5] A conceivable approach to these challenges and the energy expenditure of CO_2 separation could be the concept of thermochemical energy storage (TCES) when operating with the separated CO_2 and thereby, allowing for recovery of a portion of the energy invested in CO_2 capture.

Research on thermochemical energy storage has been inspired by the ready availability of waste energy and the notable temporal shifts in energy production and consumption. The goal of such technology is to re-utilize waste heat and thereby contribute to balancing the discrepancies between energy availability and demand. [1, 6, 7] According to this approach (thermal) energy is stored by means of reversible chemical reactions: An endothermic decomposition reaction charges the storage material, whereas by recombination of the former decomposition products the exothermic reaction discharges the stored energy and restores the material. [8, 9]

Carbonates have been established as suitable materials for TCES-processes (see Eq.1) [10], although to date they have predominantly been investigated for medium- and high-temperature applications, especially in combination with concentrating solar power plants. [11, 12]

$$MeCO_3 + \Delta H \leftrightarrow MeO + CO_2 \quad (1)$$

For TCES-systems $CaCO_3$, $PbCO_3$ and, recently, $SrCO_3$ have been considered. [12] Most efforts focused on $CaCO_3$, especially due to its potential for atmospheric CO_2 sequestration. [13]

$CaCO_3$ provides reversible decarbonatization / carbonatization with an energy storage potential of 178 kJ mol^{-1}. [12] Although fully reversible, an initial drawback was the limited cycle stability which could be overcome by dotation of the material with $CaTiO_3$. [14] Subsequent studies focused on improving the of reactivity by using CaO nanoparticles [15] or composite materials with Si. [16] Recently, zirconia-stabilized SrO / $SrCO_3$ was reported readily reversible and cyclable material for high-temperature TCES for temperatures around 1200 °C. [17] Also Cerussite ($PbCO_3$) offers attractive cycle stability [18, 19] with an energy content of 88 kJ mol^{-1} [12], due to the inherent toxicity of the materials involved, for technological applications environmentally more benign materials are required.

On the basis of attempts to decrease greenhouse gas emissions by carbon dioxide fixation *via* the carbonatization of metal oxides, [20-22] and the highly promising mineralization of CO_2, [4] we considered a novel approach to TCES-processes using CO_2: instead of applying high temperatures, moderate temperatures combined with higher pressures should result in carbonatization of metal oxides.

In this case, CO_2separated from fossil-fuel power plant waste gas could be stored in form of carbonates, which release thermal energy on their formation due to exothermic carbonatization reactions. Only compression of gas separated would be needed, which is in many cases could be easily accomplished with the available infrastructure. The use of environmentally harmless oxide / carbonate pairs would also allow for relatively simple disposal of the separated carbon dioxide.

For this purpose, in the present work, a systematic database survey was undertaken to identify potentially suitable carbonate materials complementing the currently known examples. [23] The feasible candidates were selected according to their energy content and their theoretical equilibrium temperature. The selected materials were investigated with respect to their carbonatization behavior at temperatures below 100 °C and at pressures of 55 bar and 110 bar to show the feasibility of the low temperature carbonatization systems. The current *in-situ* powder X-Ray diffraction (P-XRD) study and following carbonatization experiments in a reactor demonstrated that in the presence of moisture higher pressures can replace high temperatures for successful carbonatization of pure metal oxides.

2. Experimental Methodology

2.1 Material

The metal oxides used for carbonatization were prepared by thermal decomposition of the corresponding metal carbonates at the temperatures determined by thermogravimetric analysis (see table A1). This approach was selected to avoid potential influence of sample history on the carbonatization process.

2.2 X-Ray Powder Diffraction

The powder X-ray diffraction measurements were carried out on a PANalytical X'Pert Pro diffractometer in Bragg-Brentano geometry using Cu $K_{\alpha 1,2}$ radiation and an X'Celerator linear detector with a Ni-filter. For the *in-situ* experiments an Anton Paar XRK 900 reaction chamber was used. The sample consists of a 4 mm thick layer of oxide-powder-sample with a diameter of 10 mm and is mounted on a hollow ceramic powder sample holder, allowing for complete perfusion of the sample with the reactive gas. The reaction chamber allows operation between 25 °C and 900 °C and pressures up to 10 bar. For the carbonization experiments the pressure in the sample chamber was adjusted to 8 bar, maintaining a constant flow through the chamber of 0.2 L CO_2 min^{-1}. To investigate the carbonatization in the presence of moisture, the CO_2 was passed through an external moisturiser. The CO_2 is bubbled through a 20 cm high water tank followed by a droplet-separator before contacting the sample in the reaction chamber. At the entry of the reaction chamber the gas had a dew-point temperature of 23.2 °C. Considering the gas temperature of 25 °C, this corresponds to a water vapour loading of 0.25 g h^{-1}.

The sample temperature is controlled directly by a NiCr-NiAl thermocouple and direct environmental heating, operable at heating-rates between 0.1 K min^{-1} and 150 K min^{-1}. The reactive gas flow was set to 0.2 L min^{-1}, unless otherwise stated. The diffractograms were evaluated using the PANalytical program suite HighScorePlus v3.0d. A background correction and a $K_{\alpha 2}$ strip were performed. Phase assignment is based on the ICDD-PDF4+ database, the exact phase composition was obtained by Rietveld-refinement in the program suite HighScorePlus v3.0d.

2.3 Carbonatization in the reactor

For the carbonatization of metal oxides in a reactor at higher CO_2 pressures, a small amount of the metal oxide (around 50 mg) was placed in a glass-vial with perforated cap to avoid cross-contamination. The reactor was pressurized with CO_2 at 55 bar unless otherwise stated, controlling the internal pressure with the reactor's integrated manometer. The carbonatization was aborted after the specified reaction time by release of CO_2 pressure.

For the reactions at elevated temperatures the reactor was loaded with the samples, placed in an oven having the desired temperature and kept there for 1 h to equilibrate. Then 55 bar of CO_2 were charged and the reactor kept for the specified reaction time in the oven. Due to the thermal expansion a final internal pressure of 110 bar was reached. Again, the carbonatization was aborted by release of CO_2.

For all experiments requiring moisture approximately 0.1 ml H_2O was sprayed into the sample vials.

3. Results and Discussion

The carbonate systems for the intended low-temperature carbonatization study under elevated CO_2 pressure were selected from the HSC chemistry database using a systematic search algorithm[23] and are listed in table 1.

Table 1. Selected carbonate materials, ranked according to their theoretical energy density

Reaction	Theoretical equilibrium temperature [°C]	Theoretical energy density [GJ m^{-3}][a]
$CaMg(CO_3)_2 \rightarrow CaO + MgO + 2\ CO_2$	1152	4.52
$CaCO_3 \rightarrow CaO + CO_2$	1433	4.49
$MgCO_3 \rightarrow MgO + CO_2$	851	3.58
$MnCO_3 \rightarrow MnO + CO_2$	890	3.22
$ZnCO_3 \rightarrow ZnO + CO_2$	668	2.94
$CoCO_3 \rightarrow CoO + CO_2$	728	2.90
$FeCO_3 \rightarrow FeO + CO_2$	720	2.69

[a] The numerical values are based on the HSC Chemistry database.

$NiCO_3 \rightarrow NiO + CO_2$	655	2.31
$PbCO_3 \rightarrow PbO + CO_2$	858	2.07

To study the carbonatization reaction of those materials, the corresponding metal oxides (see materials and methods) were treated with CO_2 under various conditions initially small samples were monitored by *in-situ* P-XRD and larger samples were subsequently treated in a larger reactor to understand the carbonatization behavior under higher pressures than were possible in the P-XRD cell.

3.1 In-situ carbonatization in the P-XRD

The well-known carbonatization of calcium oxide [5, 13] was utilized to establish the viability of monitoring carbonatization reaction progress by *in-situ* P-XRD. Applying 8 bar CO_2 (under dynamic conditions the maximum pressure possible in the reaction chamber) and temperatures between room-temperature and 600 °C revealed that for dry CO_2 no carbonatization reaction occurred. As described in many cases in the literature, hydroxides are used for carbonatization studies and even the low-temperature carbonatization of $Ca(OH)_2$ was only successful in the presence of moisture. [24] The impact of moisture on the carbonatization of metal oxides can be attributed to traces of liquid water on the oxide surface, enhancing carbonatization by dissolution of the CO_2, as well as by formation of hydroxyl groups on the oxide surface promoting the carbonatization step. [25, 26] Therefore, for all further reactions a moisturizer was implemented in the setup between CO_2 tank and reaction chamber.

Using wet CO_2, having a dew-point temperature of 23.2 °C for the carbonatization, for a pressure of 1 bar CO_2 no carbonatization, but conversion of the CaO to $Ca(OH)_2$, was observed (see Fig.2). The rapid hydration of CaO in the presence of moisture has been extensively studied. [27] At pressures of 3 bar and 8 bar after a reaction time of 120 minutes 11.8 % and 33.8 % $CaCO_3$ in the presence of $Ca(OH)_2$ were obtained. The change in the phase composition over the 120 minutes reaction time is plotted in figure 1.

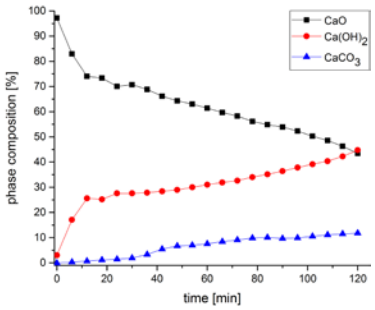

Figure 1a. Carbonatization of CaO at 3 bar

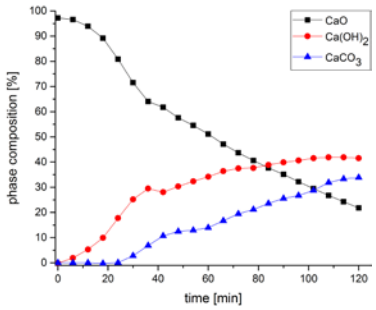

Figure 1b. Carbonatization of CaO at 8 bar

For the reaction under 3 bar CO_2 the intermediate hydroxide formation occurred faster than for the same experiment using 8 bar CO_2, indicating a notable impact of the water partial pressure on the formation of the hydroxide intermediate. At 8 bar the initial hydroxide formation is retarded, affecting also the carbonatization rate. To increase the completeness of the reaction longer carbonatization times were considered. Nevertheless, after 24 h the final phase composition was comparable to those observed after 2 h. This suggests the system is approaches an equilibrium state under these conditions.

Since the final composition of the product contains a significant amount of $Ca(OH)_2$ in spite of the application of a large excess of reactant (CO_2) it seems likely, that a passivating carbonate layer forms on the surface of the particles and prevents further carbonatization. In literature, issues with conversion and surface passivation have been described. These effects could be circumvented by modification of the particle morphology or reactor setup. [12] Similar approaches or a different setup could be considered to increase the overall carbonatization yield. However, although repetition of the reaction at 100 °C did not significantly increase the final conversion, the formation of an excess of $Ca(OH)_2$ could be suppressed.

Based on the promising initial results described above, the prospective metal oxides to be examined were subjected to *in-situ* carbonatization in the P-XRD cell. An overview of the outcomes of these *in-situ* experiments is given in figure 2.

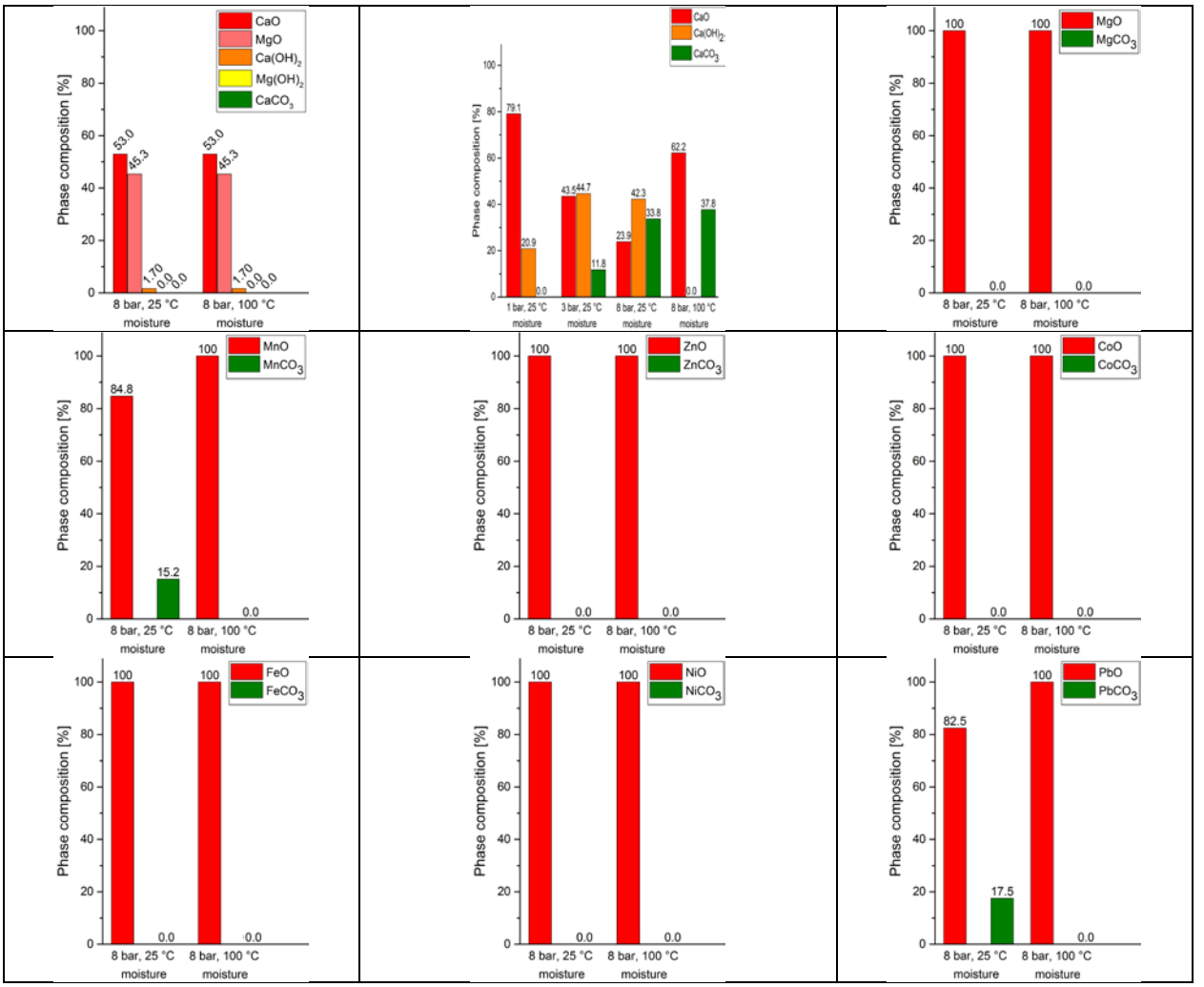

Figure 2. Final phase composition of the in-situ carbonatization under various conditions, ranked by their theoretical energy density (The original diffractograms summarized as histogram-plots are represented in Fig.A1-A9)

Aside from CaO, only MnO and PbO showed any reactivity towards CO_2 under the conditions applied. Interestingly, for neither MnO nor PbO was any intermediate hydroxide formation observed. Whether or not the carbonatization process in these cases does not involve a hydroxide phase or the reaction of the intermediate hydroxide with CO_2 is faster than the P-XRD timescale, will be the subject of future investigations. Carbonate yields of 15.2 % (MnO) and PbO (17.5 %) were limited to 25 °C, as for 100 °C only the metal oxide could was found. Compared to the partially successful monitoring of carbonatization of CaO by *in-situ* P-XRD the reactivity of the other metal oxides towards carbonatization under these conditions was disappointing.

3.2 Carbonatization in the reactor

To investigate the carbonatization behavior of metal oxides under higher CO_2 pressures, a reactor setup allowing pressures up to 55 bar (25 °C) and 110 bar (60 °C) under static conditions was chosen. The resulting phase composition was determined after the reaction by P-XRD. For each of the selected oxides, 4 different experiments were performed, establishing the effect of moisture and temperature on the carbonatization process. In figure 3, the resulting phase compositions are reported.[b]

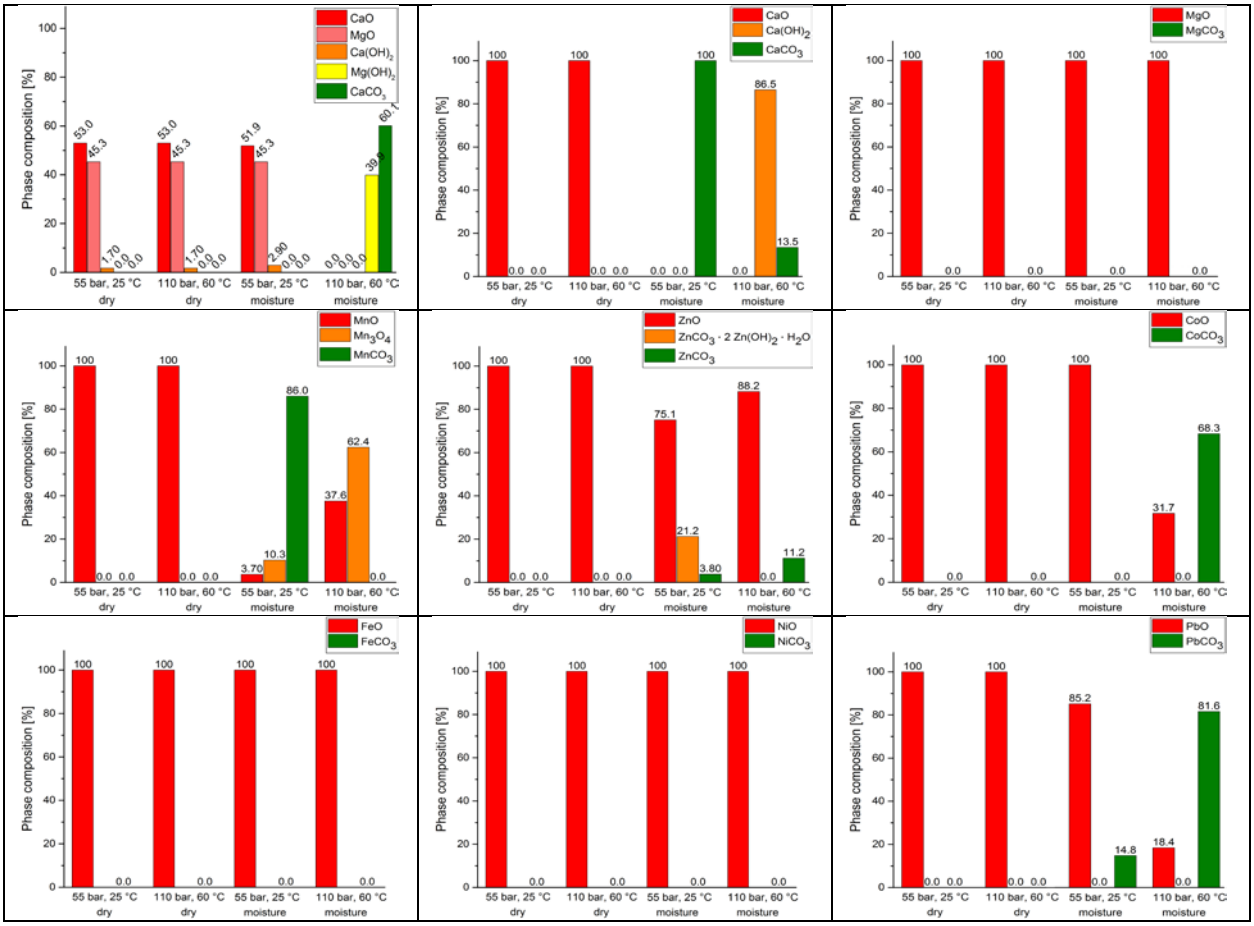

Figure 3. Final phase composition after 2 h for the carbonatization experiments in the reactor (oxides ranked by their theoretical energy density. The original diffractograms summarized here as histogram-plots are represented Fig.A10-A18)

Similarly to the *in-situ* P-XRD experiments, at higher pressures moisture was also identified as a crucial component for successful carbonatization. Under dry conditions the initial phase composition was retained. Whereas most of the materials test were not carbonatized in the *in-situ* P-XRD setup, in the case of higher pressures in the reactor only MgO, FeO and NiO failed to react. These results are in good agreement with other carbonatization studies, in which

[b] Based on the appearance of the diffractograms the presence of any amorphous material – which should give rise to a higher background or line broadening effects – could be excluded.

MgO has been carbonatized at high temperature [28], or for a longer time. [29, 30] Also in reports on basaltic-CO_2 fixation, FeO present in olivine- was inert under the carbonatization conditions applied. [30]

A sample of dolomite was nearly unaffected by carbonatization with moisture at room-temperature, but at 60 °C full carbonatization of the CaO fraction occurred. Concomitantly, the MgO was hydrated to $Mg(OH)_2$, still indifferent towards carbonatization. Carbonatization of CaO at 55 bar, 25 °C was highly successful, as after 2 h complete conversion was achieved. In this case, an increase in temperature was obstructive, preventing complete carbonatization of the intermediately formed $Ca(OH)_2$.

In the case of MnO, 55 bar CO_2, 25 °C led to a carbonatization yield of 86 %. In contrast, an increased temperature led to the unprecedented and reproducible formation of 62.4 % Mn_3O_4 after 2 h, presumably as product of MnO oxidation by CO_2. Aside from CaO, the 86 % yield of $MnCO_3$ was the highest observed in the series.

For the carbonatization of ZnO at 25 °C the double-salt $ZnCO_3 \cdot 2Zn(OH)_2 \cdot H_2O$ was identified as an intermediate phase. At higher temperatures only $ZnCO_3$ was found, due to immediate conversion of the intermediate carbonate-hydroxide phase.

CoO and PbO also revealed significant carbonatization behavior on increased temperature, yielding 68.3 % of $CoCO_3$ and 81.6 % of $PbCO_3$, respectively. At 25 °C no conversion was observed for CoO, and for PbO only a small amount of the carbonate phase (14.8 %) could be observed evidenced.

In comparison to the *in-situ* experiments monitored by P-XRD, in all cases improved reactivity was achieved by carbonatization in the reactor. For the carbonatization of PbO at 55 bar and 25 °C a lower carbonate content was observed compared to experiments in the P-XRD setup. Considering that moisture plays a crucial role in all carbonatization experiments, it seems comprehensible that lower pressures can effectively promote the carbonatization process.

4. Conclusion

Material and feasibility studies on the carbonatization of metal oxides at elevated CO_2 pressure and temperatures below 100 °C both in presence or absence of moisture have been carried out. The reactions were performed *in-situ* in the P-XRD (8 bar, variable temperatures) and in a pressure reactor (55 bar, 25 °C; 110 bar, 60 °C). For all used materials and conditions moisture revealed as crucial for carbonatization, as under dry conditions always the initial oxide-phase composition was retained.

Only for CaO, MnO and PbO could the formation of a carbonate phase be observed in relatively small amounts under *in-situ* P-XRD conditions. In contrast, higher pressures (55 bar, 25 °C and 110 bar, 60 °C) enabled carbonatization of CaO in dolomite, CaO, MnO, ZnO, CoO and PbO within 2 h. Of the selected metal oxides, only for CaO at 55 bar, 25 °C was complete carbonatization achieved. Comparably high carbonatization yields were obtained for MnO (86 % $MnCO_3$) at 55 bar, 25 °C, as well as for CoO ($CoCO_3$ 68.3 %) and PbO (81.6 % $PbCO_3$), both at 110 bar, 60 °C.

Based on these initial carbonatization results, intensified contact between metal oxide and moisture should allow for even higher carbonatization yields. Investigations regarding calorimetric data of the carbonatization and reaction rates for CaO, MnO, CoO and PbO under the applied conditions are the subject of on-going studies.

5. Acknowledgement

This work was financially supported by the Austrian Research Promotion Agency (FFG Forschungsförderungsgesellschaft), project 845020, 841150 and project 848876. The X-Ray center (XRC) of the Vienna University of Technology provided access to the powder X-Ray diffractometer.

6. Appendix

Table A1. Decomposition temperatures of metal carbonates determined via thermogravimetry

Carbonate	Decomposition temperature to MeO*
$CaCO_3$	785 °C

$CoCO_3$	370 °C
Dolomite	815 °C
$FeCO_3$	550 °C
$MnCO_3$	450 °C
$MgCO_3$	480 °C
$NiCO_3$	375 °C
$PbCO_3$	375 °C
$ZnCO_3$	370 °C

* The given decomposition temperature refers not to the peak onset, but to the final flattening, stating complete decarbonation yielding the respective metal oxides MeO

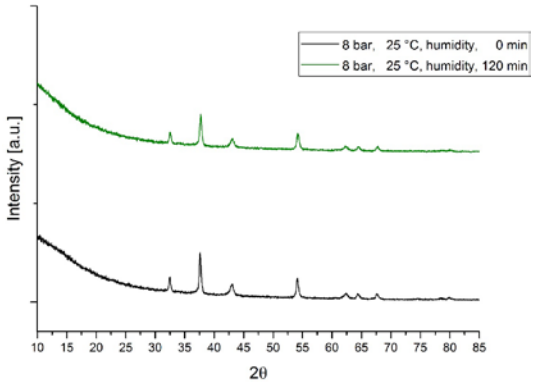

Figure A1. Diffractograms for *in-situ* re-carbonation forming Dolomite

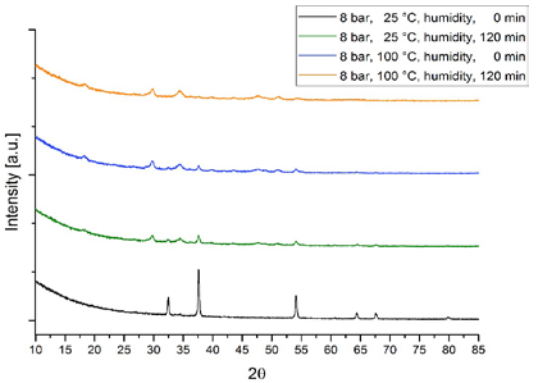

Figure A2. Diffractograms for *in-situ* carbonation of CaO into $CaCO_3$

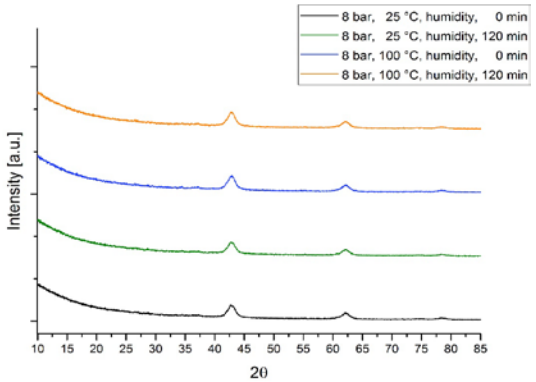

Figure A3. Diffractograms for *in-situ* carbonation of MgO into $MgCO_3$

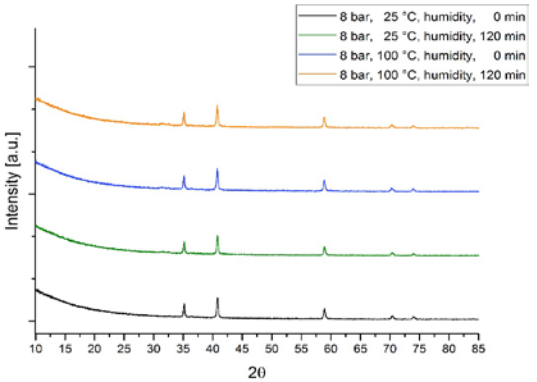

Figure A4. Diffractograms for *in-situ* carbonation of MnO into $MnCO_3$

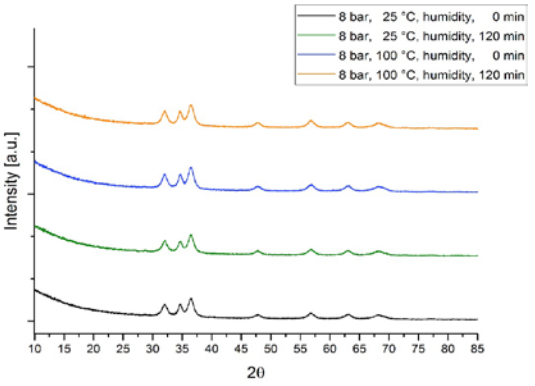

Figure A5. Diffractograms for *in-situ* carbonation of ZnO into $ZnCO_3$

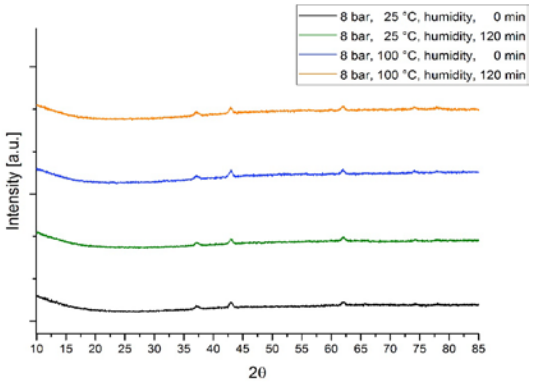

Figure A6. Diffractograms for *in-situ* carbonation of CoO into $CoCO_3$

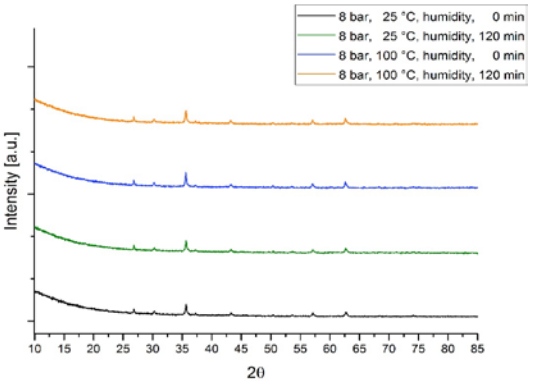

Figure A7. Diffractograms for *in-situ* carbonation of FeO into $FeCO_3$

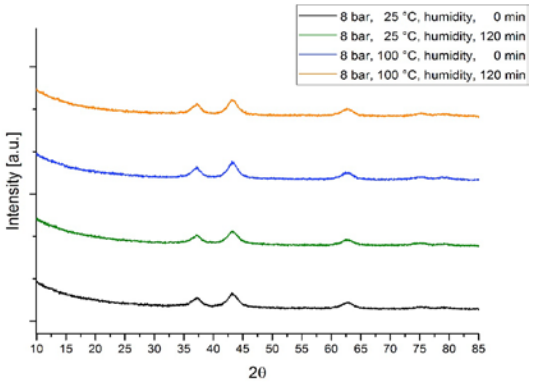

Figure A8. Diffractograms for *in-situ* carbonation of NiO into $NiCO_3$

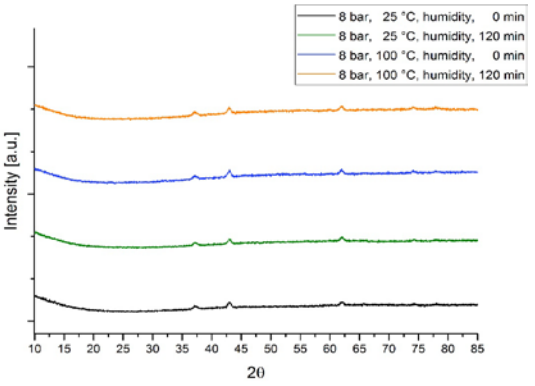

Figure A9. Diffractograms for *in-situ* carbonation of PbO into $PbCO_3$

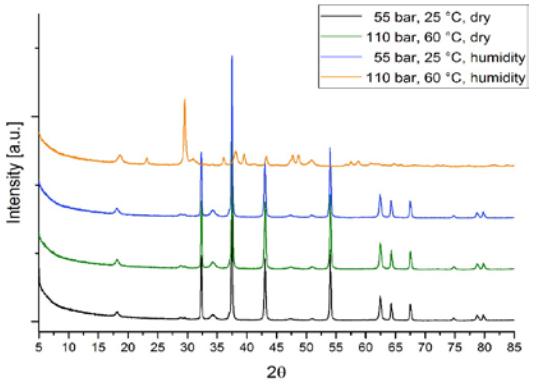

Figure A10. Diffractograms for reactor re-carbonation forming Dolomite

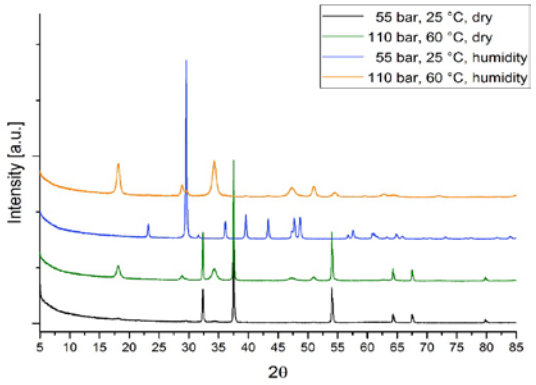

Figure A11. Diffractograms for reactor carbonation of CaO into $CaCO_3$

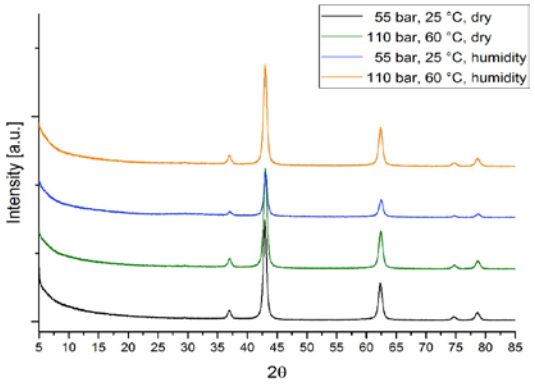

Figure A12. Diffractograms for reactor carbonation of MgO into $MgCO_3$

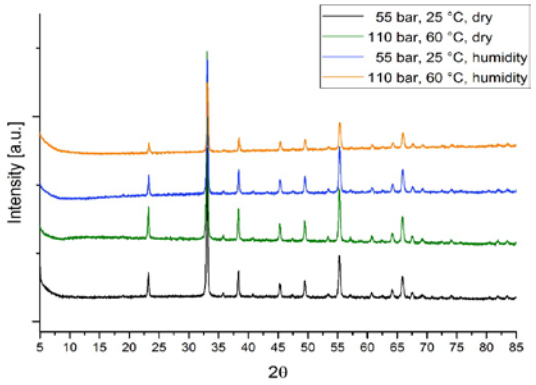

Figure A13. Diffractograms for reactor carbonation of MnO into $MnCO_3$

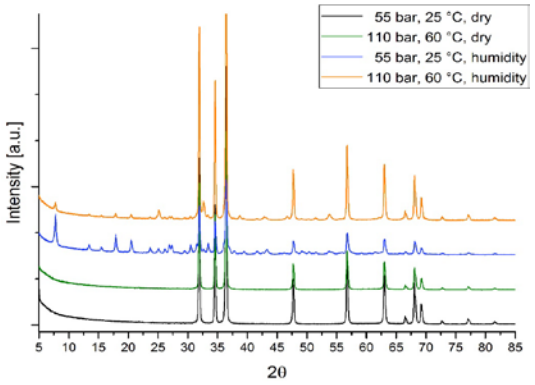

Figure A14. Diffractograms for reactor carbonation of ZnO into $ZnCO_3$

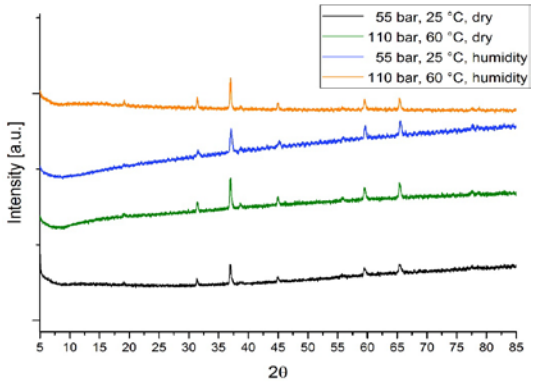

Figure A15. Diffractograms for reactor carbonation of CoO into $CoCO_3$

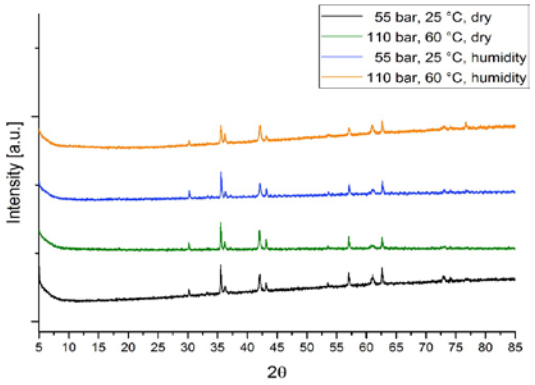

Figure A16. Diffractograms for reactor carbonation of FeO into $FeCO_3$

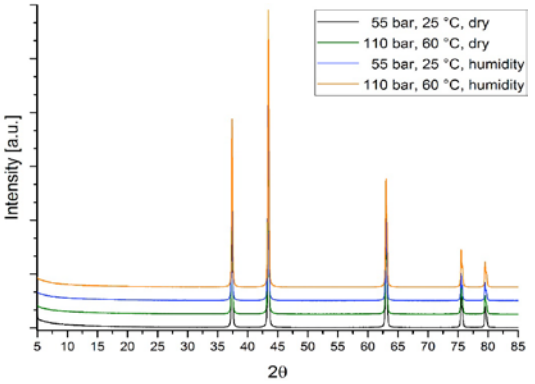

Figure A17. Diffractograms for reactor carbonation of NiO into $NiCO_3$

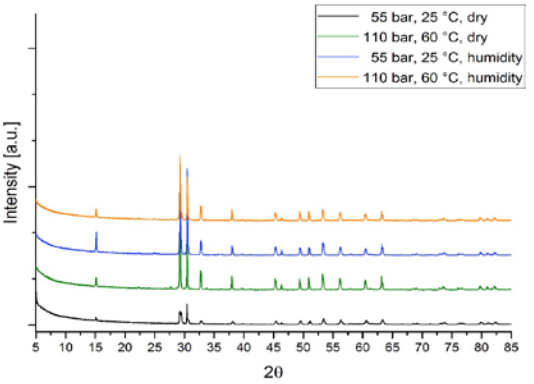

Figure A18. Diffractograms for reactor carbonation of PbO into $PbCO_3$

6. References

[1] IEA, Co-generation and Renewables. Solutions for a low-carbon energy future, https://www.iea.org/publications/freepublications/publication/co-generation-and-renewables-solutions-for-a-low-carbon-energy-future.html, (2011).
[2] U.N. Treatie, Paris agreement, No. 54113, , (2015).
[3] U. Nations, Kyoto protocol, (1997).
[4] J.M. Matter, M. Stute, S.O. Snaebjornsdottir, E.H. Oelkers, S.R. Gislason, E.S. Aradottir, B. Sigfusson, I. Gunnarsson, H. Sigurdardottir, E. Gunnlaugsson, G. Axelsson, H.A. Alfredsson, D. Wolff-Boenisch, K. Mesfin, D.F.d.l.R. Taya, J. Hall, K. Dideriksen, W.S. Broecker, Rapid carbon mineralization for permanent disposal of anthropogenic carbon dioxide emissions, Science, 352 (2016) 1312-1314.
[5] E.D. H. Herzog, E. Adams, CO2 Capture, Reuse, and Storage Technologies for Mitigating Global Climate Change. A White Paper, Final Report No. DE-AF22-96PC01257; U.S. Department of Energy: Washington, DC, (1997).
[6] IEA, Heating without global warming: Market developments and policy considerations for renewable heat, (2014).
[7] D. Rahm, Sustainable Energy and the States, Essay on Politics Markets and Leadership, McFarland, North Carolina, 1st edt. (2002).
[8] S.M. Hasnain, Review on sustainable thermal energy storage technologies, Part I: heat storage materials and techniques, Energy Conversion and Management, 39 (1998) 1127-1138.
[9] R.Z.W. T. Yan, T. X. Li, L.W.Wang, Ishugah T. Fred, A review of promising candidate reactions for chemical heat storage, Renewable and Sustainable Energy Reviews, 43 (2015) 13-31.
[10] A.H. Abedin, M.R. Rosen, A Critical Review of Thermochemical Energy Storage Systems, The Open Renewable Energy Journal, 4 (2011) 42-46.
[11] K. Kyaw, H. Matsuda, M. Hasatani, Applicability of Carbonation/Decarbonation Reactions to High-Tempereture Thermal Energy Storage and Temperature Upgrading, Journal of Chemical Engineering of Japan, 29 (1996) 119-125.
[12] P. Pardo, A. Deydier, Z. Anxionnaz-Minvielle, S. Rougé, M. Cabassud, P. Cognet, A review on high temperature thermochemical heat energy storage, Renewable and Sustainable Energy Reviews, 32 (2014) 591-610.
[13] J.C. Abanades, The maximum capture efficiency of CO2 using a carbonation/calcination cycle of CaO/CaCO3, Chemical Engineering Journal, 90 (2002) 303-306.
[14] M. Aihara, T. Nagai, J. Matsushita, Y. Negishi, H. Ohya, Development of porous solid reactant for thermal-energy storage and temperature upgrade using carbonation/decarbonation reaction, Applied Energy, 69 (2001) 225-238.
[15] K.V. Valavala, H. Tian, S. Sinha, Carbonation Characteristics of Isolated Calcium Oxide Nanoparticles for Thermal Energy Storage, Nanoscale and Microscale Thermophysical Engineering, 17 (2013) 204-215.
[16] Y. Álvarez Criado, M. Alonso, J.C. Abanades, Composite Material for Thermochemical Energy Storage Using CaO/Ca(OH)2, Industrial & Engineering Chemistry Research, 54 (2015) 9314-9327.
[17] N.R. Rhodes, A. Barde, K. Randhir, L. Li, D.W. Hahn, R. Mei, J.F. Klausner, N. AuYeung, Solar Thermochemical Energy Storage Through Carbonation Cycles of SrCO3/SrO Supported on SrZrO3, ChemSusChem, 8 (2015) 3793-3798.
[18] Y. Kato, N. Harada, Y. Yoshizawa, Kinetic feasibility of a chemical heat pump for heat utilization of high-temperature processes, Applied Thermal Engineering, 19 (1999) 239-254.
[19] Y. Kato, D. Saku, N. Harada, Y. Yoshizawa, Utilization of high temperature heat from nuclear reactor using inorganic chemical heat pump, Progress in Nuclear Energy, 32 (1998) 563-570.
[20] K.S. Lackner, CLIMATE CHANGE: A Guide to CO2 Sequestration, Science, 300 (2003) 1677-1678.
[21] J.S.F. Keith P. Shine , Kinfe Hailemariam, Nicola Stuber, Alternatives to the Global Warming Potential for Comparing Climate Impacts of Emissions of Greenhouse Gases, climatic change, 68 (2005) 281-302.
[22] L. Reich, Towards Solar Thermochemical Carbon Dioxide Capture via Calcium Oxide Looping: A Review, Aerosol and Air Quality Research, (2014).
[23] M. Deutsch, D. Müller, C. Aumeyr, C. Jordan, C. Gierl-Mayer, P. Weinberger, F. Winter, A. Werner, Systematic search algorithm for potential thermochemical energy storage systems, Applied Energy, 183 (2016) 113-120.

[24] S.-M. Shih, C.u.-S. Ho, Y.-S. Song, J.-P. Lin, Kinetics of the Reaction of Ca(OH)2with CO2at Low Temperature, Industrial & Engineering Chemistry Research, 38 (1999) 1316-1322.
[25] D.T. Beruto, R. Botter, Liquid-like H2O adsorption layers to catalyze the Ca(OH)2/CO2 solid–gas reaction and to form a non-protective solid product layer at 20°C, Journal of the European Ceramic Society, 20 (2000) 497-503.
[26] K. Van Balen, Carbonation reaction of lime, kinetics at ambient temperature, Cement and Concrete Research, 35 (2005) 647-657.
[27] V.S. Ramachandran, P.J. Sereda, R.F. Feldman, Mechanism of Hydration of Calcium Oxide, Nature, 201 (1964) 288-289.
[28] K. Yamauchi, N. Murayama, J. Shibata, Absorption and Release of Carbon Dioxide with Various Metal Oxides and Hydroxides, Materials Transactions, 48 (2007) 2739-2742.
[29] V. Morales-Flórez, A. Santos, I. Romero-Hermida, L. Esquivias, Hydration and carbonation reactions of calcium oxide by weathering: Kinetics and changes in the nanostructure, Chemical Engineering Journal, 265 (2015) 194-200.
[30] O. Sissmann, F. Brunet, I. Martinez, F. Guyot, A. Verlaguet, Y. Pinquier, D. Daval, Enhanced Olivine Carbonation within a Basalt as Compared to Single-Phase Experiments: Reevaluating the Potential of CO2Mineral Sequestration, Environmental science & technology, 48 (2014) 5512-5519.